

0358

REPORT DOCUMENTATION PAGE

Public reporting burden for this collection of information is estimated to average 1 hour per response, including the time for reviewing instructions, searching existing data sources, gathering and maintaining the data needed, and completing and reviewing the collection of information. Send comments regarding this burden estimate or any other aspect of collection of information, including suggestions for reducing this burden, to Washington Headquarters Services, Directorate for Information Operations and Reports, 1215 Jefferson Davis Highway, Suite 1204, Arlington, VA 22202-4302, and to the Office of Management and Budget, Paperwork Reduction Project (0704-0188), Washington, DC 20503.

1. AGENCY USE ONLY (Leave blank)	2. REPORT DATE 3/96	3. REPORT TYPE AND DATES COVERED Final
----------------------------------	------------------------	---

4. TITLE AND SUBTITLE 75 Micron YAG-Alumina Eutectic Fiber	5. FUNDING NUMBERS C F49620- 95-C-0065
---	---

6. AUTHOR(S) Joseph M. Collins

7. PERFORMING ORGANIZATION NAME(S) AND ADDRESS(ES) Saphikon, Inc. 33 Powers Street Milford, NH 03055	8. PERFORMING ORGANIZATION REPORT NUMBER AFM-F-I
---	---

9. SPONSORING/MONITORING AGENCY NAME(S) AND ADDRESS(ES) AFOSR Directorate of Aerospace and Materials Science 110 Duncan Ave., Room B115 Bolling AFB, DC 20332-0001	10. SPONSORING/MONITORING AGENCY REPORT NUMBER 95-C-0065
---	---

11. SUPPLEMENTARY NOTES

12a. DISTRIBUTION/AVAILABILITY STATEMENT Approved for public release, distribution unlimited	19960726 081
--	--------------

13. ABSTRACT (Maximum 200 words) Crystal growth experiments were conducted to test the application of the Edge-defined Film-fed Growth (EFG™) technique to the growth of 75 μm single crystal yttrium aluminum garnet - alumina eutectic fiber (YAE). A total of 21 growth runs were made and fibers were produced with lengths up to 12 meters long. Diameters of the fibers ranged from 70 μm to 100 μm and growth speeds ranged from 169 to 677 μm/min. Fiber microstructures were eutectic with both Chinese script and lamellar morphologies present. The best room temperature tensile strengths were obtained from run #116 with an average tensile strength of 3.19 GPa (463 Ksi) for 20 tests while the highest strength sample tested at 1094°C was from run #106 with a tensile strength of 1.74 GPa (253 Ksi) for 20 tests.
--

14. SUBJECT TERMS Fiber, Ceramic, Composite, YAG, Alumina, Eutectic	15. NUMBER OF PAGES 13	16. PRICE CODE
--	---------------------------	----------------

17. SECURITY CLASSIFICATION OF REPORT Unclassified	18. SECURITY CLASSIFICATION OF THIS PAGE Unclassified	19. SECURITY CLASSIFICATION OF ABSTRACT Unclassified	20. LIMITATION OF ABST U
---	--	---	-----------------------------

75 MICRON YAG-ALUMINA EUTECTIC FIBER

AFOSF/NA

Directorate of Aerospace and Materials Science

CONTRACT F49620-95-C-0065

Reference: Saphikon PO# 30302

ATTN: Dr. Alexander Pechinik

Bolling AFB DC 20332-0001

Final Technical Report

For The Period of August 1995 to January 1996

Submitted by:

J. M. Collins

Saphikon, Inc.

33 Powers Street

Milford, NH 03055

1. ABSTRACT

Crystal growth experiments were conducted to test the application of the Edge-defined Film-fed Growth (EFGTM) technique to the growth of 75 μm single crystal yttrium aluminum garnet - alumina eutectic fiber (YAE). A total of 21 growth runs were made and fibers were produced with lengths up to 12 meters long. Diameters of the fibers ranged from 70 μm to 100 μm and growth speeds ranged from 169 to 677 $\mu\text{m}/\text{min}$. Fiber microstructures were eutectic with both Chinese script and lamellar morphologies present. The best room temperature tensile strengths were obtained from run #116 with an average tensile strength of 3.19 GPa (463 Ksi) for 20 tests while the highest strength sample tested at 1094°C was from run #106 with a tensile strengths of 1.74 GPa (253 Ksi) for 20 tests.

Table of Contents

1. ABSTRACT.....	2
2. INTRODUCTION	4
3. BACKGROUND.....	5
4. EXPERIMENTAL PROCEDURES.....	5
<i>4.1. Materials.....</i>	<i>5</i>
<i>4.2. Growth Setup.....</i>	<i>5</i>
<i>4.3. Growth Procedures.....</i>	<i>7</i>
5. PHASE I EXPERIMENTAL RESULTS	7
<i>5.1. Preliminary Growth Trials</i>	<i>7</i>
<i>5.2. DOE Growth Trials</i>	<i>7</i>
<i>5.3. Confirmation Run</i>	<i>8</i>
<i>5.4. Tensile Test Data</i>	<i>8</i>
<i>5.5. Characterization:.....</i>	<i>9</i>
<i>5.6. Discussion:</i>	<i>9</i>
6. FUTURE WORK.....	10
7. CONCLUSIONS.....	10
8. REFERENCES.....	11
9. APPENDICIES	12
<i>9.1. Appendix A. Growth Run Summary.....</i>	<i>12</i>
<i>9.2. Appendix B. Tensile test data.....</i>	<i>13</i>

2. INTRODUCTION

Advanced engines inevitably require high operating temperatures to satisfy efficiency and performance goals in an increasingly competitive economic environment. This means that combustor and exhaust system components can operate at temperatures $> 2400^{\circ}\text{F}$ (1316°C) and become limited by critical material properties such as creep, thermal fatigue, oxidation and thermal shock resistance. Thermo-oxidative stability, material cost and component manufactured cost are equally important. The application of ceramic matrix composites (CMC's) to these applications is considered essential for achieving the property and performance goals stated above.

Refractory ceramic materials which are capable of operation at the very high temperatures of interest, $>1370^{\circ}\text{C}$ ($>2500^{\circ}\text{F}$), generally fall into one of two categories: materials which are inherently stable to oxidation (i.e. oxides), or oxidizable materials which form protective oxide films of silica. Recent theoretical¹ and experimental^{1,2} work has shown that composites based on oxidizable phases within dense oxide matrices demonstrate poor oxidation resistance. The above references clearly indicate that any reinforcement for an oxide matrix must itself be inherently stable against oxidation. The only materials which meet this criterion are oxides and noble metals; however, noble metals are impractical due to their poor high temperature mechanical properties and their very high densities. **This leaves only the oxides as reinforcement candidates for oxide matrix composites.**

Presently, several types of continuous oxide fibers are commercially available. Unfortunately, the majority of these fibers are produced either from organometallic precursors (sol-gel) or by the extrusion and sintering of fine powders. The resultant fibers are typically contain thermally unstable amorphous or metastable phases. These microstructures make the fibers highly susceptible to strength degradation via crystallization or grain growth. All polycrystalline fibers show strength degradation above 800°C , and little or no strength above 1200°C . Only oxide single crystal fibers maintain a significant portion of their strength at 1370°C and above. The relatively good high temperature strength of the Saphikon fibers is a direct result of their stable, single crystal structure, which eliminates the degradation mechanism mentioned above.

Even though the Saphikon EFG single crystal alumina fiber is stable at elevated temperatures, other properties make it less desirable as a fiber reinforcement. These are primarily the rapid strength loss at moderate temperatures ($\sim 400^{\circ}\text{C}$)³ and the very directional nature of the creep properties of sapphire.⁴ These limitations have led to the investigation of alternate fiber compositions which have the desirable qualities of sapphire but improve on its deficiencies. Foremost among these alternatives is the EFG $75\ \mu\text{m}$ YAG-Alumina Eutectic fiber (YAE). This composition has been shown to be very stable at elevated temperatures and mechanical testing of $150\ \mu\text{m}$ YAE fibers yielded elevated temperature (1094°C (2000°F)) strengths which were $\sim 33\%$ stronger than sapphire fibers.⁵ Furthermore the creep properties of this fiber were comparable to sapphire⁵ and should show little variation with crystal orientation due to the very high creep resistance of the yttrium aluminum garnet (YAG) phase.

3. BACKGROUND

The YAE fibers are grown using the Edge-defined Film-fed Growth (EFG™) process. The EFG™ setup is comprised of a refractory metal crucible for containing the high purity feedstock material, with a capillary/die arrangement configured within the crucible. Induction heating is used to melt the feedstock, which rises in the capillary to the die tip, as shown in Figure 1. The outside shape of the die tip defines the shape of the crystal. For fiber growth, the die shape is circular, with a single drilled capillary in the center of the circle. Rectangular, square, and complex cross sectional shapes can also be grown with the EFG process.

A crystallographically oriented seed fiber is guided into contact with the tip. Once the tip of the seed is melted by contact with the die tip, the seed is pulled upward at a controlled rate. The crystal can then be grown continuously, with the solidifying region at the die tip being continuously replenished via capillary flow from the crucible. The entire hot zone can be enclosed in an argon atmosphere. A continuous belt puller and spooler arrangement is used to allow for the growth of fibers hundreds of meters long.

4. EXPERIMENTAL PROCEDURES

4.1. Materials

Starting materials were 99.995% Al_2O_3 from flame fusion boules and 99.99% YAG powder ($\text{Y}_3\text{Al}_5\text{O}_{12}$). In some runs the charge was melted in a vacuum in the molybdenum and tungsten setup before growth. Charge weights were typically ~50 grams. Two compositions were grown in this program. They were 18.5 mole % Y_2O_3 : 81.5 mole % Al_2O_3 and 20 mole % Y_2O_3 : 80 mole % Al_2O_3 .

4.2. Growth Setup

The growth setup was fabricated from molybdenum and tungsten. The crucible was 1.75 inches in diameter and 2 inches high. A thin shield, 0.5 mm (0.02 in), was used as a radiation shield for the top of the setup. The die was fabricated from two pieces, the lower die a slotted rectangular piece of molybdenum to allow the melt to rise to the die array, and the die array itself. The die array was produced by laser drilling. The crucible was supported on tungsten pins, which in turn rested on a graphite pedestal. The circumference of the crucible was surrounded with a graphite heat shield.

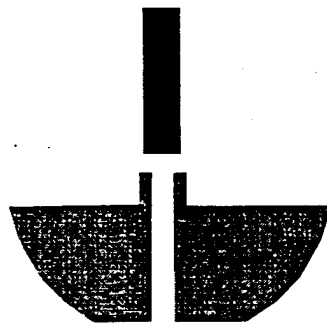
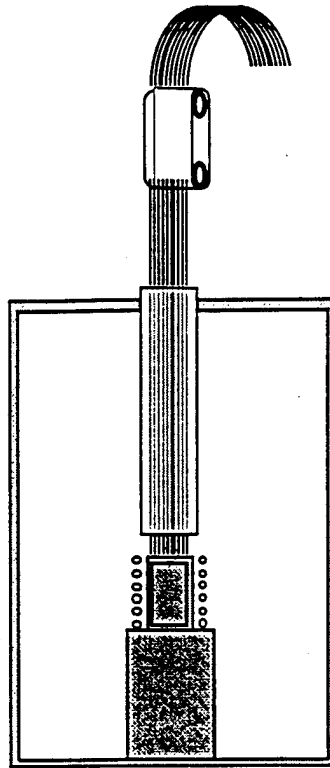


Figure 1. EFG fiber growth schematic

4.3. Growth Procedures

The setup, described above, was heated by a 10 KHz RF induction heating system within a metal walled water cooled chamber. An induction coil was located inside the chamber and the setup rested on a copper hearth plate. The growth atmosphere was argon with flow rates of ~2 liters/minute. Seeding was accomplished by dipping a sapphire seed into the melt at the die top and withdrawing it to form a fiber of the melt. Adjustments were made to the pull rate and temperature to control the fiber diameter.

5. PHASE I EXPERIMENTAL RESULTS

5.1. Preliminary Growth Trials

A total of nine growth runs, #101-#109, were made to determine the appropriate growth parameters. Appendix 9.1 lists the details of these growth runs and appendix 9.2 lists the tensile strength data for these growth runs. At the end of these growth runs it was deemed that the growth process window had been suitably characterized to allow the Design of Experiments (DOE) matrix to be started.

5.2. DOE Growth Trials

The subsequent 11 runs, #110-#120, were then used to complete a three factor full factorial experiment with two replications for a total of 16 trials. The factors investigated were pull rate, composition and vacuum melting and the response variable was room temperature tensile strength. Table I gives the experimental settings for this experiment and the resulting RT tensile strengths. Two of the trials from one growth run were not completed due to growth difficulties: These trials were to be a replication for run #112, and so for the analysis of the experiment the RT tensile strength values were set to same values as those from run #112. The experiment was then analyzed using a non-parametric rank order statistical procedure. The results of this analysis indicated that only one factor, the pull rate, was significant to >95%. The analysis indicated that higher pull rates corresponded to higher RT tensile strengths. The other two factors and all interactions were not significant at a 95% threshold.

The two other primary factors, though they were not significant for RT tensile strength, were considered to be important for other quality characteristics. Specifically, the vacuum melting was considered desirable for pre-conditioning the melt for growth and further analysis would be needed to quantify this characteristic. The composition may have a strong influence on the creep and stability of the fibers. It is expected that as more yttrium oxide is added to the melt, there will be a corresponding increase in the amount of the YAG (yttrium aluminum garnet) phase which is one of the most creep resistant oxides. It is hoped that by increasing the YAG phase in

the fiber a corresponding improvement in the creep properties of the fiber will result. Another benefit of the additional YAG phase may be better stability of the microstructure at elevated temperatures. Both of these results will have to be verified by experiment data in future work, though it is encouraging that they do not significantly affect the RT mechanical properties of these fibers.

Exp. #	Run #	Pull Rate ($\mu\text{m}/\text{sec}$)	Composition (mol%)	Vacuum Melt (Y/N)	RT Tensile Strength (GPa (Ksi))	Comments
1	110	169	18.5	Y	1.59 (231)	
3	111	169	20.0	N	1.75 (254)	
5	112	169	18.5	N	1.67 (242)	
7	113	169	20.0	Y	1.47 (213)	
9	114	169	18.5	Y	1.39 (202)	
----	115	169	18.5	N	----	Not completed
14	116	169	20.0	Y	1.48 (215)	
15	120	169	20.0	N	1.40 (203)	
2	110	339	18.5	Y	2.10 (305)	
4	111	339	20.0	N	2.00 (290)	
6	112	339	18.5	N	1.76 (255)	
8	113	339	20.0	Y	1.88 (273)	
10	114	339	18.5	Y	1.95 (283)	
----	115	339	18.5	N	----	Not completed
13	116	339	20.0	Y	1.96 (284)	
16	120	339	20.0	N	1.68 (244)	

5.3. Confirmation Run

One confirmation run was made based on the results of the experiment. This experiment produced well over the 100 meters of fiber required for the program deliverable. This run grew quite well and will be provided to the Contract Monitor for evaluation.

5.4. Tensile Test Data

Appendix 9.2 list the tensile test data for all of the experimental runs which were tested. Table II lists the highest values extracted from that appendix. These values came from only two growth trials. Both of these fibers were grown at some of the highest growth rates, 423 and 677 $\mu\text{m}/\text{sec}$, used in this program. It can be seen that, for the growth trial 116 especially, the RT tensile strengths are quite high, approaching those of sapphire fibers (~ 3.4 GPa). The elevated temperature tensile strength values are also quite high, but the effect of pull rate does not appear to correlate as well as it does in the RT tensile strength data. It does appear that pull rate is a contributing factor to the elevated temperature strength, but other unknown factors also appear to be important. The elevated temperature (1095°C (2000°F)) test strengths of the YAE fibers are $\sim 50\%$ higher than those of sapphire and it is expected that there will not be a significant strength

drop in the temperature range of 400-800°C as is seen in sapphire fibers. Previous work with 125 μm YAE fibers demonstrated no loss of strength at intermediate temperatures.

Run ID	Test Temp. (°C (°F))	Pull Rate (μm/sec)	Number of Tests	Strength (GPa (Ksi))	Std. Deviation (GPa (Ksi))
106	RT	423	20	2.14 (310)	0.38 (56)
106	2000 (1094)	423	20	1.74 (253)	0.11 (16)
116R1.6	RT	677	19	3.19 (463)	0.77 (112)
116E1.6	2000 (1094)	677	10	1.58 (230)	0.19 (28)

5.5. Characterization:

A limited amount of SEM and optical microscopy characterization was done on the YAE fibers. Both Chinese script and lamellar type microstructures were observed using the SEM. These microstructures are consistent with previous work with 125 μm YAE fibers. Due to the limited time available no detailed examinations were made of grain sizes or of the effect of pull rate on the grain sizes. It is expected that future work will involve a close examination of the grain size and morphologies.

Optical microscopy was used successfully to determine the bulk morphology of the fibers. It was previously determined that using a unique lighting technique to illuminate the fiber cross-section it was possible to differentiate regions of lamellar morphology from those having a Chinese script morphology. Our examinations of these fibers showed that they were all single morphology fibers of either lamellar or Chinese script with no dual morphology sections. NASA Lewis determined that dual morphology microstructures showed significant strength reductions during high temperature soaking.⁶

5.6. Discussion:

The YAE 75 μm fiber has been developed to the extent that it can be grown successfully and the fiber produced shows significant property improvements over sapphire fiber at elevated temperatures and most likely enhances the intermediate temperature mechanical properties. Furthermore, the growth window is very similar to 125μm sapphire fiber and so entails little extra cost for the added benefits.

The results of the DOE analysis indicated that pull rate had a significant effect on the RT tensile strength of the YAE fiber while vacuum pre-melting and composition had no detectable effects on the RT tensile strengths. This data was corroborated by other tensile data reported above which showed the highest tensile strength fibers were grown at the highest growth rates. Pre-melting was considered desirable as a conditioning step before fiber growth was started and may enhance the manufacturing capability of the fiber. The DOE did not show any effect of this process step on the RT tensile strength. In addition, the composition was considered important

for improving the creep properties of the fiber. It is a significant result that the composition did not directly affect the RT tensile strength as it could have a beneficial effect on the creep properties with no negative consequences on the tensile properties. This remains to be proven.

Overall the 75 μm YAE fiber was quite straightforward to grow and provides significant property benefits over 125 μm sapphire fiber. There is a large amount of additional investigation needed to optimize the fiber. The Phase I program demonstrated the ability to produce the fiber and generated a limited amount of tensile strength data. Furthermore, pull rate was identified as a significant variable having a strong effect on the RT tensile strength. The other two factors and the interactions were not found to be significant and may be examined for their effect on other quality characteristics.

6. FUTURE WORK

The recommended approach for future work would entail three areas:

- 1.) Optimize the growth process for the 75 μm YAE fiber identifying the best process settings to grow the fiber and which yield the best mechanical properties.
- 2.) Characterize the fibers over a range of temperatures for tensile strength, creep and phase stability.
- 3.) Initiate a pilot plant run campaign to demonstrate the capability to produce significant quantities of the fiber.

7. CONCLUSIONS

The feasibility of growing 75 μm YAE fibers was demonstrated and multiple runs were made where fibers were grown over one meter long. The tensile strength of the YAE fiber was quite good especially at 1094°C (2000°F) where it was ~50% higher than a comparable sapphire fiber. The result of the DOE was that of the three factors studied, only the pull rate had a significant influence on the RT tensile strengths and that higher growth rates produce higher tensile strength fiber. Further work needs to be done to optimize the fiber composition and the process growth parameters as well as to characterize the fiber more extensively.

8. REFERENCES

1. K. L. Luthra and H.D. Park, "Chemical Compatibility in Ceramic Composites," AFWAL-TR-89-6009.
2. M.B. Boron , M.K. Brun and L.E. Szala, "Kinetics of Oxidation of Carbide and Silicide Dispersed Phases in Oxide Matrices," *Adv. Ceram. Mater.*, 3(5) 491-97, 1988.
3. P. Shahinian, "High-Temperature Strength of Sapphire Filament," *J. Am. Ceram. Soc.*, 54 (1) 67-68, 1971.
4. L.E. Jones and R.E. Tressler, "The High Temperature Creep Behavior of Oxides and Oxide Fibers," NASA Contractor Report #187060, Jan. 1991.
5. Private communication with Dr. Ali Sayir of NASA Lewis Research Center.
6. Private communication with Dr. Ali Sayir of NASA Lewis Research Center.

9. APPENDICIES

9.1. Appendix A. Growth Run Summary

Run ID	Date Grown	Pull Rate ($\mu\text{m}/\text{sec}$)	# of Fibers Seeded	Length (m)	Comments
101	8/6/95	635	3	1.7	Spooling problems
102	8/8/95	----	----	----	Seeding and Flooding Problems
103	8/10/95	635	5	1.6	
104	8/21/95	----	----	----	Die not feeding
105	8/22/95	423	1	0.55	
106	8/30/95	423	1	15.18	
107	9/6/95	339-423	15	10.88	
108	9/13/95	----	----	----	Setup blobbed
109	9/14/95	339	12	5	
110	9/20/95	169-339	30	3.39	First DOE exp. run
111	9/22/95	169-339	20	3.07	Second DOE exp. run
112	9/25/95	169-339	14	3.66	Third DOE exp. run
113	9/29/95	169-339	30	3.11	Fourth DOE exp. run
114	10/2/95	169-339	28	3.18	Fifth DOE exp. run
115	10/4/95	169-339	30	0.98	Unsuccessful DOE exp. run
116	10/9/95	169-339	30	4.76	Seventh DOE exp. run
117	10/13/95	169-339	30	1.93	Unsuccessful DOE exp. run
118	11/1/95	----	----	----	Unsuccessful DOE exp. run
119	11/6/95	169-339	26	0.49	Unsuccessful DOE exp. run
120	11/29/95	169-339	29	3.34	Eight DOE exp. run
121	1/5/95	423	25	12.33	Confirmation run

9.2. Appendix B. Tensile test data.

Run ID	Test Temp. (°C (°F))	Number of Tests	Strength (GPa (Ksi))	Std. Deviation (GPa (Ksi))
106	RT	20	2.14 (310)	0.38 (56)
106	2000 (1094)	20	1.74 (253)	0.11 (16)
107	RT	30	1.81 (262)	0.31 (44)
107	2000 (1094)	30	1.49 (216)	0.14 (21)
109	RT	30	1.90 (275)	0.37 (53)
109	2000 (1094)	30	1.50 (218)	0.15 (22)
110R4	RT	20	1.59 (230)	0.28 (41)
110R8	RT	20	2.10 (304)	0.41 (59)
110E4	2000 (1094)	20	1.32 (191)	0.13 (19)
110E8	2000 (1094)	20	1.40 (202)	0.25 (36)
111R4	RT	20	1.75 (253)	0.13 (18)
111R8	RT	20	2.00 (290)	0.24 (35)
111E4	2000 (1094)	20	1.23 (178)	0.13 (19)
111E8	2000 (1094)	20	1.06 (153)	0.16 (23)
112R4	RT	19	1.67 (242)	0.28 (40)
112R8	RT	19	1.76 (255)	0.48 (70)
112E4	2000 (1094)	19	1.27 (184)	0.15 (21)
112R8	RT	20	1.76 (255)	0.48 (70)
113R4	RT	18	1.47 (213)	0.48 (70)
113R8	RT	19	1.88 (272)	0.36 (52)
114R4	RT	20	1.39 (202)	0.45 (66)
114R8	RT	20	1.95 (283)	0.34 (54)
116R4	RT	18	1.48 (215)	0.31 (45)
116R8	RT	19	1.96 (285)	0.33 (49)
116R1.6	RT	19	3.19 (463)	0.77 (112)
116E1.6	2000 (1094)	10	1.58 (230)	0.19 (28)
120R4	RT	19	1.40 (203)	0.28 (40)
120R8	RT	20	1.68 (243)	0.39 (56)